



Published in final edited form as:

Exp Neurol. 2020 January ; 323: 113088. doi:10.1016/j.expneurol.2019.113088.

Vitronectin mitigates stroke-increased neurogenesis only in female mice and through FAK-regulated IL-6

Cuihong Jia, Matthew P. Keasey, Hannah M. Malone, Chiharu Lovins, Theo Hagg*

Department of Biomedical Sciences, Quillen College of Medicine, East Tennessee State University, Johnson City, Tennessee, USA, 37614

Abstract

Vitronectin (VTN) is a blood protein produced mainly by the liver. We show that VTN leaks from the bloodstream into the injury site and neighboring subventricular zone (SVZ) following ischemic stroke (middle cerebral artery occlusion, MCAO) in adult mice. MCAO is known to increase neurogenesis after stroke. VTN inhibits this response in females, but not in males, as shown by ~70% more stroke-induced SVZ neurogenesis in female VTN^{-/-} mice at 14 d. In female VTN^{-/-} mice, stroke-induced expression of interleukin-6 (IL-6) at 24 h was reduced in the SVZ. The closely related leukemia inhibitory factor (LIF) or pro-neurogenic ciliary neurotrophic factor (CNTF) were not affected. The female-specific effect of VTN on IL-6 expression was not due to sex hormones, as shown by ovariectomy and castration. IL-6 injection next to the SVZ reversed the MCAO-induced increase in neurogenesis seen in VTN^{-/-} mice. Our in vitro and vivo data suggest that plasma VTN activates focal adhesion kinase (FAK) in the SVZ following MCAO, which reduces IL-6 expression in astrocytes but increases it in other cells such as microglia/macrophages. Inducible conditional astrocytic FAK deletion increased MCAO-induced IL-6 expression in females at 24 h and blocked MCAO-induced neurogenesis at 14 d, confirming a key detrimental role of IL-6. Collectively, these data suggest that leakage of VTN into the SVZ reduces the neurogenic response to stroke in female mice by promoting IL-6 expression. Reducing VTN or VTN signaling may be an approach to promote neurogenesis for neuroprotection and cell replacement after stroke in females.

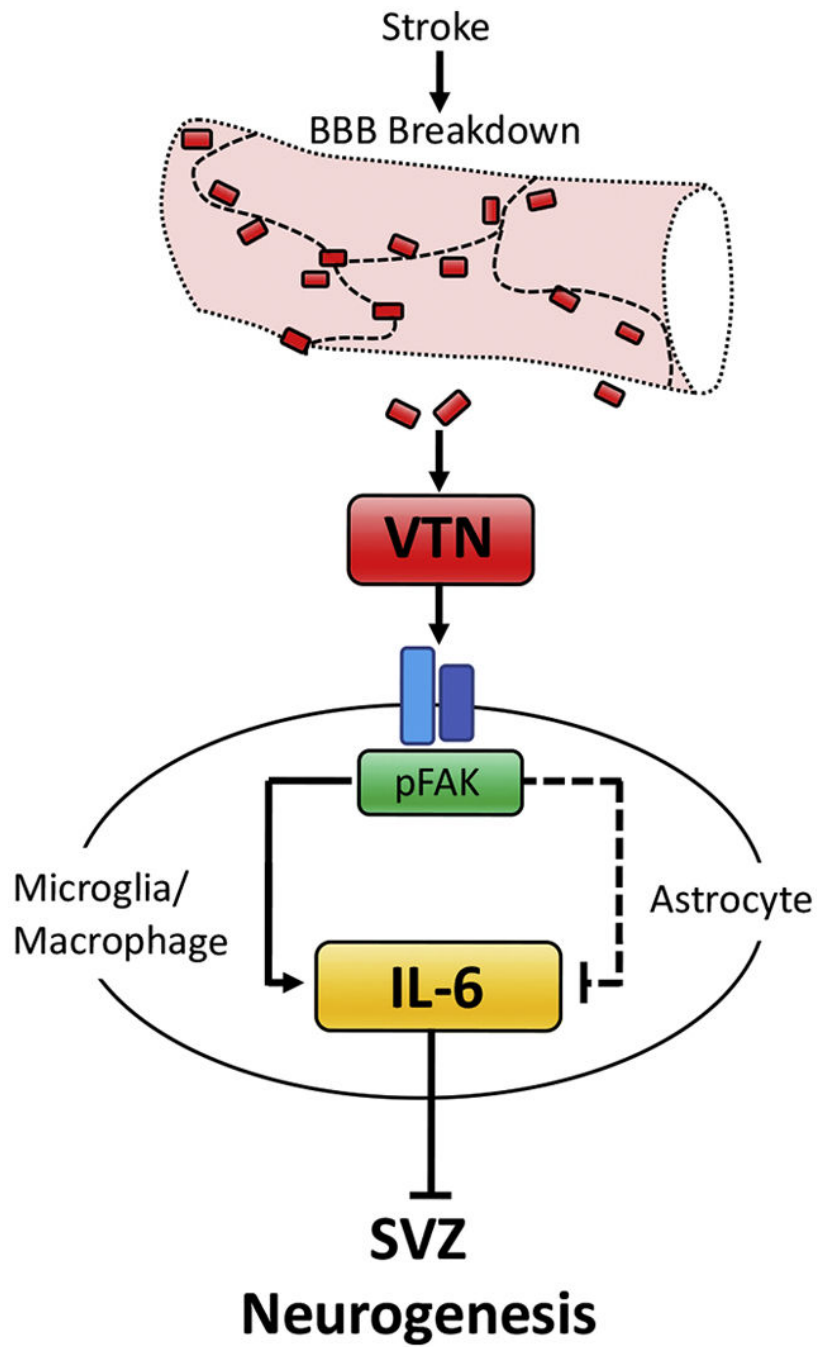
Graphical Abstract

*For correspondence: Dr. Theo Hagg, Department of Biomedical Sciences, PO Box 70582, East Tennessee State University, Johnson City, TN 37614, hagg1@etsu.edu, Phone number: 423-439-6294.

Author contributions: C.J. and T.H. designed research, C.J., M.H. M.P.K. and C.L. performed the experiments, C.J. and T.H. analyzed the data, and C.J., M.P.K. and T.H. interpreted the data and wrote the paper.

Conflict of interest: The authors declare no competing financial interests.

Publisher's Disclaimer: This is a PDF file of an unedited manuscript that has been accepted for publication. As a service to our customers we are providing this early version of the manuscript. The manuscript will undergo copyediting, typesetting, and review of the resulting proof before it is published in its final form. Please note that during the production process errors may be discovered which could affect the content, and all legal disclaimers that apply to the journal pertain.



Keywords

astrocyte; cytokines; focal adhesion kinase; neurogenesis; ischemic stroke; vitronectin

Introduction

Ischemic stroke is well-known to increase normally occurring neurogenesis in the forebrain SVZ and dentate gyrus in rodents (Arvidsson et al., 2002; Gotts and Chesselet, 2005a; Kang

et al., 2013; Kernie and Parent, 2010; Parent et al., 2002) and primates (Lichtenwalner and Parent, 2006; Tonchev et al., 2003; Yamashima et al., 2004). Newly formed neuroblasts migrate into the penumbra around the primary injury site, and are thought to be beneficial for neuroprotection, neuroplasticity and neuronal cell replacement (Cook et al., 2017; Gots and Chesselet, 2005b; Lichtenwalner and Parent, 2006; Ohab and Carmichael, 2008; Ourednik et al., 2002; Zhang et al., 2016). Regular astrocytes are densely packed in the SVZ (Emsley and Hagg, 2003; Yang et al., 2008) and clearly play a role in regulating neurogenesis by producing, for example, FGF2 (Mudo et al., 2007) and LIF (Banner et al., 1997). We have shown in adult mice that the increase in MCAO stroke-induced SVZ neurogenesis is predominantly mediated by increased expression of CNTF (Kang et al., 2013), which is produced exclusively by astrocytes in the CNS, including the SVZ (Emsley and Hagg, 2003; Yang et al., 2008). Like others (Liu and Chopp, 2016; Verkhratsky and Nedergaard, 2018), we (Jia et al., 2018) view astrocytes as good targets for developing treatments after stroke and other neurological disorders. In mice, robust increases in SVZ neurogenesis after stroke is delayed by a week compared to the increases in CNTF, suggesting that there are mechanisms counteracting its pro-neurogenic effects. Among potential candidates are the closely related cytokines, IL-6 and LIF which promote neural stem cell self-renewal at the expense of neural progenitor formation and differentiation (Bauer and Patterson, 2006; Bowen et al., 2011; Covey et al., 2011; Gregg and Weiss, 2005; Pitman et al., 2004; Shimazaki et al., 2001; Storer et al., 2018). Little is known about the roles of LIF and IL-6 in regulating neurogenesis after MCAO (Bauer et al., 2007; Erta et al., 2012). Both activated astrocytes and microglia can produce cytokines such as LIF and IL-6 (Banner et al., 1997; del Zoppo et al., 2007; Taylor and Sansing, 2013; Van Wagoner and Benveniste, 1999) and do so after stroke (Strecker et al., 2011). Astroglial-specific IL-6 knockout in female, but not male, mice is protective against a multiple sclerosis EAE inflammation model (Erta et al., 2016), but this has not been tested after stroke. The individual contributions of these cells to production of these cytokines and neurogenesis after stroke is not clear. Understanding the individual roles of these cytokines may identify new therapeutic targets and strategies to increase neurogenesis earlier or longer in order to reduce neurological deficits after stroke.

VTN is a blood protein produced mainly by the liver and leaks into the brain after injury. We and others have recently found that it is also produced by pericytes (He et al., 2016; Jia et al., 2019b) and that it promotes CNTF, LIF and IL-6 expression in naïve mice (Jia et al., 2019b). VTN is deposited in the brain after ischemic stroke in male baboons where it activates microglia (del Zoppo et al., 2012). Activated microglia and infiltrating macrophages contribute to detrimental inflammation after stroke in part by producing cytokines and MMPs (del Zoppo et al., 2007; Taylor and Sansing, 2013). Less is known about astrocytes after stroke. Little is known about the role and signaling mechanisms of VTN after ischemic stroke. VTN is well-known to bind to integrin receptors which generally activate signaling mediators such as Focal Adhesion Kinase, FAK (Giancotti and Ruoslahti, 1999; Humphries et al., 2006). Surprisingly, intracerebral injected recombinant human VTN (rhVTN) induces cytokines by inhibiting FAK in the astrocytes in naïve mice (Jia et al., 2019b). A better understanding of the role of this signaling pathway in astrocytes which can

produce CNTF, LIF and IL-6 is expected to provide more selective and pharmacological therapeutic strategies.

Here, we investigated the role of VTN in regulating MCAO-induced cytokine expression and neurogenesis in the SVZ using female and male VTN^{-/-} and inducible astrocytic FAK null mice.

Materials and methods

Animals and experimental design

In total, we used 306 adult mice and ~50 pups. Adult C57BL/6 (JAX Stock 000664), pregnant female C57BL/6, VTN (JAX Stock 004371) and GFAP-cre breeders (B6.Cg-Tg(GFAP-cre/ERT2)505Fmv/J, JAX Stock 012849) were from The Jackson Laboratory. The FAK-flox mice breeders (B6;129X1-*Ptk2^{tm1Lfr}*/Mmucd, RRID:MMRRC_009967-UCD) were from the MMRRC at the University of California, Davis. Experimental mice were produced by breeding heterozygous mice and characterized as described in detail before (Jia et al., 2019b). To induce cre-lox gene excision, tamoxifen (T5648, Sigma) was injected i.p. at 50 mg/kg, twice a day, for five days. Fourteen days later, such mice were used for MCAO experiments. Tamoxifen induced an increase in body weight compared to no increase with oil control injections ($10.3 \pm 3.0\%$ vs. $-1.1 \pm 4.2\%$, $p < 0.05$, $n=16,14$) over 5 d of injection and 14 d post-injection period before the MCAO (data not shown). However, there was no difference in body weight gain in the conditional knockout and control FAK-lox mice treated with tamoxifen ($5.0 \pm 2.9\%$ vs. $3.3 \pm 3.3\%$, $n=19,22$). Some groups of mice were ovariectomized or castrated and used for MCAO experiments 2 weeks later, as indicated. SVZ tissue was collected fresh at 24 h after MCAO for cytokine mRNA and protein analyses. In mice with i.v. injection of rhVTN, SVZ tissue was collected at 28 h after MCAO. For histological analyses, mice were processed at 24 h, 28 h or 14 d. All procedures and postoperative care were approved by the University Committee on Animal Care and complied with the NIH Guide on Care and Use of Animals.

MCAO and intrastriatal injections

A 30 min MCAO was performed as described (Kang et al., 2013) in which blood flow in the cortex was reduced to less than 20% using Doppler flowmetry and body temperature was maintained. Cortical blood flow levels before or during the MCAO were not different among C57BL/6, VTN^{+/+}, VTN^{-/-}, FAK-lox and GFAP-cre/FAK-lox mice and less than 2% on average. Sham operated animals underwent the same procedure except that the 0.21 mm thick Doccol filament was not inserted. To document VTN leakage following stroke, rhVTN (50 µg in 100 µl of saline, Sigma, SRP3186) was injected intravenously via the jugular vein at 24 h after MCAO in C57BL/6 mice or VTN^{-/-} mice. Four hours later, the mice were perfused with PBS for SVZ fresh tissue collection used in western blotting or with PBS followed by 4% paraformaldehyde for immunostaining (experimental design, Supplemental Fig. 1A). To measure MCAO-induced changes in the levels of VTN mRNA, C57BL/6 mice were perfused with PBS at 24 h after MCAO and followed by fresh SVZ tissue collection. To assess SVZ cell proliferation, BrdU (50 mg/kg, i.p.) was injected at 12, 13 and 14 days, with the last injection 2 h before processing (experimental design, Supplemental Fig. 1B).

BrdU labeling was not done during the acute phase because such BrdU-labeled neuroblasts would have migrated away by 14 days. We were interested in the longer-term effects of the early IL-6 peak expression after stroke. To investigate IL-6 effect on VTN-induced inhibition of SVZ neurogenesis in female mice, mouse IL-6 (100 ng in 1 μ l PBS, Cat# 200-06, Peprotech) or control (1 μ l PBS) was stereotactically injected into the striatum neighboring the SVZ as described before (Kang et al., 2012) in female VTN^{+/+} and VTN^{-/-} mice immediately before MCAO. Then the mice were processed for histological analysis of neurogenesis at 14 days (experimental design, Supplemental Fig. 1B). To determine the effect of plasma VTN on FAK phosphorylation in the SVZ, PBS (1 μ l), VTN^{+/+} plasma (1 μ l) or VTN^{-/-} plasma (1 μ l) was injected into the striatum next to the SVZ of VTN^{+/+} mice and fresh SVZ tissue was collected at 24 h (experimental design, Supplemental Fig. 1C). To determine the effect of FAK inhibition on MCAO-induced cytokine expression, female mice received an MCAO followed by i.p injection of saline or FAK inhibitor, FAK14 (3 mg/kg, Tocris, #3414) at 6 h when IL-6 is increasing and then SVZ tissue was collected at 24 h after MCAO.

Ovariectomy (OVX) and castration (CAS)

Females were ovariectomized and males were castrated as described previously (Jia et al., 2019a). For OVX, the oviduct and ovary on each side were first ligated with a sterile silk ligature and then removed by incisions through two 0.5 cm incisions on each side of back. For CAS, a suture was first placed around vas deferens and spermatic blood vessels on each side through a 0.5 cm midline incision in the scrotum and followed by removal of the testes. The skin and muscle were sutured afterwards. MCAO or Sham surgeries were performed 14 days after OVX or CAS.

mRNA and protein quantification

A 0.5 mm strip of SVZ-containing brain tissue was collected (Jia et al., 2018). CNTF (Mm00446373_m1), LIF (Mm00434762_g1), IL-6 (Mm00446190_m1) and GAPDH (4352932E) mRNA expression levels in RNA extracts were quantified by RT-qPCR using primers (Life Technologies) and a QuantStudio 6 Flex (Applied Biosystems) as described (Jia et al., 2018). The protein extract was dissociated in 100 μ l RIPA buffer supplemented with proteinase and phosphatase inhibitors by sonication. The protein levels of VTN, actin, phosphorylated FAK (pFAK) and total FAK were measured by western blot, as described previously (Jia et al., 2018), with mouse anti-human VTN (1:500, MAB88917, Millipore, RRID:AB 2216433), rabbit anti-GAPDH (1:2000, #5174, Cell Signaling, RRID:AB 10622025), rabbit anti-pFAK (1:1000, #3283, Cell Signaling, RRID:AB 2173659) and rabbit anti-FAK (1:1000, #3285, Cell Signaling, RRID:AB 2269034) antibody. Each sample was run in three independent gels and densitometry performed on each western blot.

Immunostaining and cell counting

Mice were perfused with ice-cold PBS followed by 4% paraformaldehyde. After cryoprotection in 30% sucrose overnight, 20 or 30 μ m coronal sections containing the SVZ were collected from the genu of the corpus callosum to the anterior commissure decussation using a cryostat or microtome. Every 6th section was stained for BrdU (1:1000, ab6326, Abcam RRID:AB 305426) followed by DAB or for BrdU and doublecortin (DCX) double

labeling (DCX, 1:500, SC-8066, Santa Cruz, RRID:AB 2088494) followed by appropriate secondary antibodies (Invitrogen), as described (Jia and Hegg, 2015; Jia et al., 2019b). Nuclei were stained with DAPI. BrdU-positive nuclei in the SVZ were counted using unbiased stereology (Kang et al., 2013) and BrdU/DCX double-labeled neuroblasts in the dorsolateral SVZ were counted manually (Jia and Hegg, 2015; Jia et al., 2019b) by researchers blinded to the treatment. To detect leaked VTN at 24 or 28 h after MCAO, 20 μ m coronal sections were stained with mouse anti-human VTN antibody (1:200, MAB88917, Millipore, RRID:AB 2216433). The immunostaining specificity was validated by replacing the primary antibody with purified isotype IgG or by staining VTN^{-/-} tissue. Some sections were stained with rabbit anti-mouse VTN antibody (1:1000, ab62769, Abcam, RRID:AB 956454, (Jia et al., 2019b). Rat anti-CD31 (1:500, #550274, BD Biosciences, RRID:AB 393571) was used to delineate endothelial cells and show perivascular VTN staining. To detect IL-6 expression in different cell types at 24 h after MCAO, 20 μ m coronal frozen sections were stained with goat anti-mouse IL-6 antibody (1:100, AF-406-NA, R&D Systems, RRID:AB 354478) combined with rabbit anti-S100 (astrocytes, instead of lowly expressed GFAP, 1:250, Z0311, Agilent, RRID:AB 10013383), rat anti-CD11b (microglia, 1:200, 14-0112-82, ThermoFisher Scientific, RRID:AB 467108), mouse anti-NeuN (neurons, 1:500, 550274, BD Biosciences, RRID:AB 393571) or rat anti-CD31 (endothelial cells) antibody. All staining was followed by appropriate secondary antibodies (Invitrogen) to visualize the positive immunofluorescent staining. The nuclei were counterstained with DAPI.

Cell culture experiments

Primary astrocytes were isolated from P0-1 day old mouse pups as previously described (Kang et al., 2012). Briefly, cortices were collected and digested in 0.25% trypsin-EDTA for 15 min at 37°C. Tissue was dissociated in DMEM with 10% serum containing DNase (1 mg/ml), centrifuged cell pellets collected and resuspended in medium containing 10% FBS [v/v], 2 mM L-Glutamine in DMEM. Cells were plated for 24 h in t75 culture flasks, washed to remove dead cells and then incubated for a further 7-10 days until confluent. After trypsinization, they were plated onto poly-D-lysine (50 μ g/ml) and laminin (50 μ g/ml) coated 6 well plates (50,000 cells/ml) for another 3 days. The cells were then treated with vehicle (culture medium plus 0.1% DMSO), vehicle plus FAK14 (10 μ M) or vehicle plus PF573228 (10 μ M, Tocris, #3239) for 4 h before RNA isolation. Cytokines were quantified by RT-qPCR by delta delta CT method and expressed relative to vehicle treated controls (n=3 independent experiments).

Statistics.

Statistically significant differences ($p < 0.05$) were determined using Graphpad Prism 7. Three or more experimental groups were analyzed by one-way ANOVA or paired one-way ANOVA with Bonferroni *post hoc* multiple comparisons, whereas two-way ANOVA with *post hoc* Tukey multiple comparisons was used for four or more groups or when two factors needed to be tested, e.g., genotypes and stroke. A Student's t-test was used to compare two groups.

Results

Blood VTN leaks into the SVZ following stroke

VTN deposits in the injured brain might derive from blood (del Zoppo et al., 2012) or resident perivascular pericytes (Jia et al., 2019b). To definitively show leakage of VTN from the bloodstream into the SVZ following stroke, PBS or rhVTN was injected i.v. into C57BL/6 mice at 24 h following MCAO. VTN protein in the SVZ, as measured by western blotting, was increased by ~20% (Fig. 1A,B; the antibody also recognized endogenous mouse VTN) 4 h after rhVTN injection. Local VTN mRNA expression in the SVZ was reduced 24 h after MCAO (Fig. 1C). Together, this suggests that i.v. injected rhVTN enters the brain following MCAO. Moreover, in VTN^{-/-} mice, i.v. injected rhVTN at 24 h following MCAO was clearly detectable in the SVZ 4 h later, as shown by immunostaining (Fig. 1D,E). Antibody specificity was confirmed by the absence of immunoreactivity in both isotype IgG-stained rhVTN-injected VTN^{-/-} mice (Fig. 1F) and VTN antibody-stained naïve VTN^{-/-} mice (Fig. 1G). Leaked plasma VTN (using another validated antibody (Jia et al., 2019b)) was present in deposits around microvessels (identified by CD31-positive endothelial cells) of the SVZ, as shown in C57BL/6 mice 24 h after MCAO (Fig. 1H-N,P). Consistent with our previous study (Jia et al., 2019b), pericytes surrounding the microvessels also expressed VTN (Fig. 1K,M), as shown by co-localization with the pericyte marker CD13 (Fig. 1N,O, arrowhead). The number of VTN-positive pericytes seemed to be reduced at 24 h after MCAO (Fig. 1J,P, arrowheads) compared to sham-operated mice (Fig. 1K,Q, arrowheads), consistent with the reduced VTN mRNA expression (Fig. 1C).

Leaked plasma VTN mitigates stroke-induced neurogenesis

In VTN^{+/+} (wildtype) mice, MCAO caused an increase from the basal level of SVZ proliferation at 14 d in both female (Fig. 2A,B) and male (Fig. 2D,E) mice, as shown by BrdU immunostaining. This increase appeared even greater in female VTN^{-/-} littermates (Fig. 2C) but not in male VTN^{-/-} littermates (Fig. 2F). BrdU/DCX double-immunofluorescent staining also showed increases after MCAO, representing an increase in neurogenesis, i.e., neuroblast formation, in both females (Fig. 2G,H) and males (Fig. 2J,K). The VTN^{-/-} females (Fig. 2I), but not VTN^{-/-} males (Fig. 2L), seemed to have increased neurogenesis.

Unbiased stereological cell counts confirmed that the MCAO-induced proliferation in the SVZ was even more increased in female VTN^{-/-} mice, almost three times which seen in sham operated mice (Fig. 3A). The stroke-induced increase in male mice was not different between VTN^{+/+} and VTN^{-/-} mice (Fig. 3B). This female-specific effect of genetic VTN deletion was also shown in BrdU/DCX counts (Fig. 3C vs. Fig. 3D), with a more than two-fold increase in neurogenesis in the VTN^{-/-} females (~180%) compared to the wildtypes (80%), suggesting that VTN suppresses MCAO-induced neurogenesis in females.

VTN induces IL-6 in the SVZ of females after stroke

At 24 h following MCAO, expression of IL-6 in the SVZ was induced ~81 fold in female VTN^{+/+} mice but only ~27 fold in female VTN^{-/-} littermates, compared to sham-operated VTN^{+/+} mice (Fig. 4A, first two columns). The IL-6 expression in female sham mice was

not different between VTN^{+/+} and VTN^{-/-} mice (data not shown). Expression of CNTF mRNA was increased 1.5 fold compared to sham-operated VTN^{+/+} female mice (Fig. 4B), and was not different in VTN^{-/-} littermates. LIF expression in the SVZ was increased by ~7.5 fold in both VTN^{+/+} and VTN^{-/-} female mice (Fig. 4C). In males, MCAO-induced IL-6 (Fig. 4E), CNTF (Fig. 4F) and LIF (Fig. 4G) expression were not significantly different between VTN^{+/+} and VTN^{-/-} mice. In sham-operated male mice, the expression of these cytokines was also not different between two genotypes (data not shown). Collectively, these data indicate that leaked plasma VTN stimulates IL-6 production following stroke in female but not male mice.

Female-specific effects of VTN are not caused by gonadal hormones.

To determine whether gonadal sex hormones interacted with the VTN genotype to cause female-specific differences in IL-6 expression in the SVZ at 24 h after MCAO, female mice were ovariectomized 2 weeks prior to MCAO. MCAO-induced IL-6 expression was comparable in both VTN^{+/+} and VTN^{-/-} mice after ovariectomy (OVX) when compared to their respective no OVX mice (Fig. 4). Further the reduction of IL-6 in the VTN^{-/-} mice was to the same extent (49%) compared to VTN^{+/+} females after OVX (Fig. 4A, second two columns), as seen in the VTN^{-/-} females without an OVX (54%, Fig. 4A, first two columns). MCAO-induced CNTF expression in both VTN^{+/+} and VTN^{-/-} females with an OVX was similar to that seen in females without an OVX (Fig. 4B). LIF expression also was increased to the same level after MCAO in VTN^{+/+} and VTN^{-/-} mice with an OVX (Fig. 4C, second two columns), and the lower averages after OVX were not significantly different from females without OVX after MCAO. Cytokine expression in female VTN^{+/+} mice with a MCAO sham operation was not significantly different with or without an OVX (Fig. 4D). Collectively, OVX did not alter the IL-6 phenotype seen in VTN^{-/-} females, suggesting that female gonadal hormones do not mediate or influence the effects of VTN on MCAO-induced IL-6.

To assess whether male gonadal hormones, such as testosterone, might be involved in masking the VTN knockout phenotype seen in females, males were castrated and received an MCAO 2 weeks later. MCAO-induced IL-6 (Fig. 4E, second two columns), CNTF (Fig. 4F, second two columns) and LIF (Fig. 4G, second two columns) expression at 24 h in the SVZ in castration (CAS) mice were not different between VTN^{+/+} and VTN^{-/-} mice. This suggests that the lack of a VTN^{-/-} phenotype in MCAO-induced IL-6 in males is not due to masking effects of male gonadal hormones. However, CAS did have substantial effects on the level of cytokine expression in MCAO males, leading to a ~85% reduction in IL-6 (Fig. 4E), and a 5-fold increase in CNTF (Fig. 4F) and 4-fold increase in LIF (Fig. 4G) expression. This effect of CAS was also seen in the sham operated male VTN^{+/+} mice (Fig. 4H). These data suggest that male gonadal hormones differentially regulate cytokine expression under normal conditions and that this is maintained following MCAO.

IL-6 injection blocks MCAO-induced neurogenesis in VTN^{-/-} females

To determine whether the much diminished induction of IL-6 in SVZ at 24 h after MCAO contributed to the greater increase in neurogenesis at 14 days in VTN^{-/-} females, IL-6 was injected in female VTN^{-/-} mice immediately before the MCAO. The single injection next

to the SVZ mimics the peak IL-6 expression at 24 h and return to baseline levels by 48-72 h seen after MCAO (Berti et al., 2002; Kang et al., 2013). At 14 days, in PBS-injected VTN^{-/-} mice, the MCAO caused a 75% increase in BrdU-labeled SVZ nuclei compared to PBS-injected VTN^{+/+} mice with an MCAO (Fig. 5A,B,D). The number of BrdU-DCX double-labeled neuroblasts was also greater in PBS-injected VTN^{-/-} compared to VTN^{+/+} mice (Fig. 5E,F,H). This confirmed the VTN^{-/-} phenotype as presented in Figure 3A,C. The IL-6-injected VTN^{-/-} mice had a similar number of BrdU-labeled nuclei in the SVZ compared to PBS-injected VTN^{-/-} mice 14 d after MCAO (Fig. 5C vs. 5B, Fig. 5D). However, they had a reduced number of BrdU-DCX-labeled neuroblasts in the SVZ (Fig. 5G vs. 5F; Fig. 5H). This suggests that the reduced acute expression of IL-6 contributes to the phenotype of more MCAO-induced neurogenesis seen in VTN^{-/-} female mice, and that IL-6 normally mitigates neurogenesis. IL-6-injected mice appeared to have BrdU-positive nuclei in the striatum close to the SVZ (Fig. 5C), suggesting that an IL-6-increased inflammatory response may have masked the IL-6-reduced neurogenesis as measured by BrdU alone (Fig 5D).

Plasma VTN activates FAK to promote stroke-induced IL-6 expression in females

VTN, like many other ECM proteins, binds to integrins and is known to stimulate downstream FAK signaling to induce IL-6 expression in vitro (Keasey et al., 2018). Here, wildtype plasma collected from VTN^{+/+} mice increased the levels of phosphorylated FAK (pFAK) in the SVZ of both naïve female and male mice at 24 h following an intrastriatal injection, as compared to PBS control injection (Fig. 6A,B). In contrast, plasma from VTN^{-/-} mice did not affect pFAK, as compared to PBS. At 24 h after MCAO, pFAK in the SVZ of female VTN^{-/-} mice was reduced as compared to their genotype shams (Fig. 6C,D). The MCAO did not affect pFAK levels in VTN^{+/+} females, suggesting that leaked plasma VTN prevents reduced FAK signaling in the SVZ following stroke. In male VTN^{+/+} and VTN^{-/-} mice, MCAO increased pFAK to a similar level compared to the VTN^{+/+} sham controls (Fig. 6E,F), suggesting that leaked VTN may not be involved.

These data are consistent with our finding that intrastriatal VTN^{+/+} but not VTN^{-/-} plasma increases SVZ IL-6 expression (Jia et al., 2019b). Here, we tested whether FAK activation mediated the MCAO-induced IL-6 in females by injecting the water-soluble FAK inhibitor, FAK14, i.p. at 6 h after MCAO in C57BL/6 mice. At 24 h, FAK14 lessened the MCAO-induced IL-6 mRNA expression in the SVZ (Fig. 6G), but did not alter the mRNA levels of CNTF (Fig. 6H) or LIF (Fig. 6I). This, suggests that activation of FAK signaling is the main mediator of MCAO-induced IL-6.

Astrocytic FAK suppresses stroke-induced IL-6 in females

Whereas, VTN stimulates IL-6 via FAK in cultured C6 astrogloma and endothelial cells (Keasey et al., 2018), in naïve mice, rhVTN injection into the brain increases IL-6 expression by inhibiting astroglial FAK (Jia et al., 2019b). Here, we show that IL-6 is, indeed, present in some astrocytes in the striatum adjacent to the SVZ at 24 h after MCAO (Fig. 7A-D, arrow) when IL-6 expression peaks (Kang et al., 2013). IL-6 was also present in some microglia/macrophages (Fig. 7E-H, arrow), but not in endothelial cells (Fig. 7I-L) or neurons (Fig. 7M-O). The antibody specificity was validated by using isotype IgG (data not

shown). IL-6 immunostaining in sham-operated mice was barely detectable (data not shown). In cultured primary mouse astrocytes, inhibition of FAK with FAK14 or PF573228 (Fig. 7P), or by siRNA knockdown (n=1, data not shown) increased IL-6 mRNA after 4 h. Together, these data suggest that FAK signaling can suppress IL-6 in astrocytes.

To determine whether and how FAK in astrocytes affect expression of IL-6 after MCAO we generated inducible GFAP-cre/FAK-lox mice and their FAK-lox control littermates. FAK gene deletion was accomplished by i.p. injection of tamoxifen for 5 days and MCAO was performed 14 days after the last injection. At 24 h after MCAO, IL-6 expression in the SVZ of female GFAP-cre/FAK-lox mice was almost twice as high as in the control FAK-lox mice (Fig. 8A). The gene deletion had no effect on the basal levels of expression as shown in sham operated mice. The expression of CNTF (Fig. 8B) and LIF (Fig. 8C) was not different in GFAP-cre/FAK-lox mice compared to the FAK-lox controls after MCAO. In males, the levels of IL-6 (Fig. 8D), CNTF (Fig. 8E) and LIF (Fig. 8F) were not affected by the astrocytic FAK gene deletion.

Compared to wildtype VTN and C57BL/6 mice, the tamoxifen-injected female and male astrocytic FAK-lox control mice had lower MCAO-induced IL-6. To exclude the possibility that tamoxifen had lasting effects on cytokine expression in the FAK-lox control mice, another group of female and male GFAP-cre/FAK-lox mice were injected i.p. with control vehicle (oil) or vehicle plus tamoxifen. Two weeks later, these mice received an MCAO. MCAO-induced IL-6 at 24 h in oil-injected GFAP-cre/FAK-lox and tamoxifen-injected FAK-lox mice was comparable in both female (Fig. 8G vs. 8A) and male (Fig. 8J vs. 8D) mice, suggesting that tamoxifen has no lasting effect on MCAO-induced IL-6. Importantly, in females, the expression of IL-6 in the SVZ was four-fold higher in tamoxifen treated mice compared to those injected with oil (Fig. 8G), confirming the findings in figure 8A. The levels of CNTF (Fig. 8H) and LIF (Fig. 8I) were not significantly different between oil and tamoxifen, mimicking the data in figure 8B and C, respectively. The cytokine expression in male GFAP-cre/FAK-lox mice injected two weeks before the MCAO with tamoxifen was not different from the oil-injected males (Fig 8J-L). Taken together, the cre-lox data suggest that FAK activation in astrocytes does not lead to increased IL-6 expression after MCAO in either females or males. However, they do not exclude the possibility that FAK signaling is reduced in astrocytes and contributes to the VTN-induced increase in IL6 specifically in females, as we showed in naïve mice (Jia et al., 2019b).

Astrocytic FAK deletion blocks stroke-induced neurogenesis in females

To determine whether the greater acute increase in IL-6 expression after MCAO in the female GFAP-cre/FAK-lox mice affected SVZ neurogenesis, another group of such females and their FAK-lox controls was analyzed 14 d after MCAO. BrdU was injected systemically over the last 50 hours. As expected (Kang et al., 2013), the number of BrdU-positive nuclei in the SVZ was increased almost two-fold in FAK-lox control mice after MCAO compared to their sham controls (Fig. 9). In sharp contrast, the number of BrdU-positive nuclei was not significantly different between the female GFAP-cre/FAK-lox with an MCAO and their sham controls, or compared to the FAK-lox (containing FAK) sham controls. This suggests

that the higher acute expression of IL-6 after MCAO (Fig. 8A,G) caused a long-lasting suppression of the stroke-induced neurogenesis.

Discussion

Blood VTN is a novel regulator of neurogenesis in females after stroke

Our study shows that VTN leaks from the bloodstream into the injured brain after stroke and only in females reduces SVZ neurogenesis by increasing stroke-induced IL-6 expression. VTN has also been shown to leak into injury sites after stroke in primates (del Zoppo et al., 2012). Clearly, VTN is not the exclusive regulator of IL-6 in females, as is evident in VTN^{-/-} mice which still have a 25-fold increase after MCAO (vs. 80 in VTN^{+/+}, Fig 4A). We also found in a collagenase hemorrhage model in the striatum, which is associated with substantial leakage of blood, that increased IL-6 expression is much reduced but not entirely blocked in VTN^{-/-} mice (Keasey et al., 2018). Thus, other blood proteins probably play a role as well, including the high concentrations of fibrinogen and fibronectin which can induce inflammation in the brain (Lominadze et al., 2010; Milner et al., 2007). VTN is the main IL-6 activator within plasma injected into naïve mice (Jia et al., 2019b) but this seems to be different after stroke. The relatively large effects of VTN we found after hemorrhagic and ischemic stroke suggest that it might be a good therapeutic target.

Most stroke studies involving the SVZ have focused on molecules that promote neurogenesis (Wiltrott et al., 2007), which include FGF2 (Mudo et al., 2007), IGF-1 (Yan et al., 2006), EPO (Tsai et al., 2006), Wnt3a ((Shruster et al., 2012; Wang et al., 2009) and angiogenic factors such as VEGF and Ang1 (Ohab et al., 2006). We have shown that CNTF mediates all of the increase in neurogenesis after an MCAO in mice (Kang et al., 2013). A few other studies have reported on negative regulators of SVZ neurogenesis after stroke, e.g., TNF α (Iosif et al., 2008). This is consistent with the findings that BBB breakdown contributes to inflammation, which is overall detrimental to neurogenesis and involve IL-6 and TNF α expression (Ekdahl et al., 2003; Monje et al., 2003). BBB breakdown can also contribute to the stroke-induced neurogenesis, most likely by leakage of circulating blood molecules, including VEGF165 (Lin et al., 2019; Lin et al., 2018). Platelet injections into the brain can promote SVZ proliferation in demyelinating injury model (Kazanis et al., 2015), suggesting that they contain proteins that induce pro-neurogenic factors such as CNTF and FGF2 or inhibit cytokines such as IL-6. Interestingly, BBB breakdown can even create new stem cell niches (Lin et al., 2015), suggesting that circulating molecules might be used to produce new cells in brain regions other than the SVZ and SGZ.

Potential VTN-related female-specific mechanisms

Surprisingly, VTN and the subsequent induction of IL-6 inhibited SVZ neurogenesis after stroke only in females. We (Jia et al., 2019b) and others (Tatar et al., 2013) have shown that baseline neurogenesis are not strikingly different between young naïve female and male mice. On the other hand, the positive role of female hormones in SVZ neurogenesis after stroke has been well documented (Suzuki et al., 2007). However, our results suggest that the female-specific detrimental effect of VTN after stroke is not related to levels of either female or male gonadal hormones. Very few other studies have documented sex specificity for

molecules other than hormones, suggesting that VTN or the cells it binds to have special properties in females. Among potential mechanisms that remain to be studied are sex differences in VTN isoforms, VTN integrin receptor expression and downstream intracellular signaling pathways. Others include the transcription factor p53 which contributes to sex dimorphism in the proliferation and cell number in the SVZ (Kim and Casaccia-Bonnet, 2009). The TNF α receptor, TNFR1, activates p53 after brain injury (Quintana et al., 2005). Interestingly, the p53 isoforms p53 α and p53 β are expressed in astrocytes and differentially regulate their IL-6 related cytotoxic effects (Turnquist et al., 2016). It will be important to determine the role of p53 in VTN-stimulated IL-6 expression and/or reduced neurogenesis. Additional molecular mechanisms underlying the female-specific effects of VTN may come from analyses of genes including *Igfbp2*, *Slco1c1*, and *Mfap2* which have functional sex differences in the expression levels in astrocytes, as identified by single cell analyses of the adult SVZ (Mizrak et al., 2019).

Acute IL-6 expression inhibits neurogenesis after stroke

Our data suggest that the sexual dimorphism in the effect of VTN on neurogenesis is due to differences in the levels of acute IL-6 expression in the SVZ that occurs over the first day after stroke and is reduced to near normal levels again at 2-3 days (Berti et al., 2002; Kang et al., 2013). IL-6, like LIF, is known to promote stem cell renewal and reduce differentiation of progenitor cells to the expense of formation of neuroblasts, i.e. neurogenesis (Bauer and Patterson, 2006; Bowen et al., 2011; Covey et al., 2011; Gregg and Weiss, 2005; Pitman et al., 2004; Shimazaki et al., 2001; Storer et al., 2018). IL-6 is believed to have an overall detrimental role during inflammation (Campbell et al., 1993; Erta et al., 2012). Others have suggested that IL-6 can have beneficial effects on neurogenesis after stroke by promoting angiogenesis (Meng et al., 2015). In apparent contrast, we find that reduced IL-6 in VTN $^{-/-}$ and increased IL-6 in astroglial FAK null females at 24 h after MCAO, result in increased and decreased stroke-induced neurogenesis, respectively. Also, our rescue experiment with injected IL-6 in VTN $^{-/-}$ mice suggest that the acute peak expression of IL-6 at 24 h after stroke has lasting inhibitory effects on SVZ neurogenesis. However, it remains to be determined when inhibition of VTN signaling would be most efficacious to promote neurogenesis after stroke.

Our results also reveal that the stroke-induced increase in CNTF which mediates the induction of neurogenesis, and LIF, which stimulates neural stem cell renewal, is not regulated by VTN. This identifies differential signaling mechanisms between these highly related cytokines as we have found in naïve mice (Jia et al., 2018). The specific effects on IL-6 expression after stroke were different from our findings in naïve VTN $^{-/-}$ mice and those injected with rhVTN, where CNTF and LIF were also increased (Jia et al., 2019b). The different cytokine expression profiles after stroke compared to naïve conditions might be explained by differences in leaked plasma VTN vs. intracerebral injection of rhVTN and/or the state of activated compared to resting astrocytes and microglia.

It remains to be determined which cell types in the brain respond to VTN with an increase in IL-6 expression. Our study showed that MCAO induced IL-6 protein expression in some astrocytes and microglia/macrophages close to the SVZ at 24 h. These cells are known to

express IL-6 under various injury conditions, including stroke (Kang et al., 2013; Lambertsen et al., 2012; Suzuki et al., 2009; Van Wagoner and Benveniste, 1999). Overexpression of IL-6 in astrocytes has been shown to inhibit hippocampal neurogenesis in naïve mice (Vallieres et al., 2002), suggesting that high IL-6 is detrimental to neurogenesis. Activation of microglia in the SVZ following stroke promotes neural stem cell proliferation and differentiation, possibly through IGF-1 (Thored et al., 2009), suggesting an overall positive role of microglia on long-term SVZ neurogenesis after stroke. However, selective elimination of microglia does not affect the number of neuroblasts that exit the SVZ and migrate into the striatum after stroke (Heldmann et al., 2011). These data suggest a complex role of astrocytes and microglia on stroke-induced SVZ neurogenesis.

FAK signaling plays a role in VTN-induced IL-6 after stroke

Wildtype, but not VTN^{-/-}, plasma injected next to the naïve SVZ caused global FAK activation as shown by western blotting. This is consistent with the finding that VTN stimulates IL-6 via FAK signaling in C6 astroglia and endothelial cell lines and knockdown of FAK blocks VTN-induced IL-6 (Keasey et al., 2018). VTN seems to be the major component of plasma that induced pFAK, as shown by the lack of activation by injected VTN^{-/-} plasma (Fig 6B). In cultured C6 cells, VTN activates pFAK much more compared to fibronectin and laminin (Keasey et al., 2018). It remains to be determined whether this relatively specific effect of VTN also exists after stroke. The results with the pharmacological FAK inhibitor after MCAO suggest that FAK activation by leaked VTN contributes substantially, although not exclusively, to the stroke-induced IL-6 expression. Activation of FAK was reduced in the SVZ of female VTN^{-/-}, but not male mice, after MCAO and occurred in concert with a decrease in IL-6 only in females. This suggests that VTN-stimulated FAK underlies the observed sex differences. The cell types mediating this effect remains to be identified but probably include microglia and/or macrophages.

In contrast, astroglial FAK seems to have the opposite effects on IL-6 expression after MCAO in females, as suggested by the selective inducible genetic knockout of FAK in astrocytes. This was supported by the finding that FAK inhibition in cultured primary astrocytes induces IL-6. If VTN reduces pFAK in astrocytes after stroke, this would explain why there were no changes in total pFAK after MCAO in wildtype female mice. Given that the increased IL-6 and blocked neurogenesis in the astrocyte FAK knockout mice were specific to females suggest that this mechanism potentially underlies the sex differences related to VTN. We do not know what predisposes female astrocytes to respond differently but this most likely includes female sex hormones during and after puberty. It is conceivable that FAK activates different downstream signaling pathways in different cell types. Lastly, our findings do not exclude the possibility that VTN, e.g., by binding to uPAR (Keasey et al., 2018), or other proteins, stimulates astroglial IL-6 after stroke and reduces neurogenesis.

Differential cytokine regulation by male hormones

Finally, although the female and male gonadal hormones did not explain the female-specific effect of VTN^{-/-} on IL-6 expression, castration had an unexpected and robust effect on cytokine expression in sham-operated mice which was retained after stroke. IL-6 was reduced to very low levels, whereas CNTF and LIF were greatly increased. This again seems

to uncover differential signaling mechanisms for these related cytokines as we have found for FAK signaling in naïve mice (Jia et al., 2018). Castration causes a doubling of proliferation in the SVZ of male mice (Tatar et al., 2013), which would be consistent with the dramatic increase in CNTF and decrease in IL-6. Whereas we have shown that increased CNTF drives neurogenesis after stroke, we have not seen such robust further increases in CNTF. This suggests that testosterone or its androgen receptors might be novel targets for enhancing neurogenesis after stroke. Supra-physiological doses of testosterone block neurogenesis after stroke (Zhang et al., 2014). However, it remains to be tested whether pharmacological inhibition of endogenous testosterone would promote neurogenesis after stroke because castration itself does not (Zhang et al., 2014).

Conclusion

Collectively, these data suggest that leakage of VTN into the SVZ reduces the neurogenic response to MCAO in female mice by promoting FAK-mediated IL-6 expression. This suggests that blocking VTN, VTN binding to integrins and downstream signaling, such as FAK, or otherwise blocking acute IL-6 expression might be strategies for further increasing neurogenesis to promote better outcomes after stroke in females.

Supplementary Material

Refer to Web version on PubMed Central for supplementary material.

Acknowledgements:

We are grateful for the technical assistance by Del Lovins, the Molecular Core Facility and Microscopy Core Facility.

Funding sources: NIH grants AG029493 and C06RR0306551, and funds from the Quillen College of Medicine at East Tennessee State University.

Abbreviation:

VTN	vitronectin
rhVTN	recombinant human vitronectin
IL-6	interleukin-6
CNTF	ciliary neurotrophic factor
LIF	leukemia inhibitory factor
FGF2	fibroblast growth factor
IGF-1	insulin-like growth factor-1
VEGF	vascular endothelial growth factor
Ang 1	angiopoietin 1
TNFα	tumor necrosis factor α

EPO	erythropoietin
ECM	extracellular matrix
BrdU	bromodeoxyuridine
DCX	doublecortin
FAK	focal adhesion kinase
pFAK	phosphorylated focal adhesion kinase
μPAR	urokinase/plasminogen activator urokinase receptor
CNS	central nervous system
SVZ	subventricular zone
SGZ	subgranular zone of hippocampus
BBB	blood brain barrier
MCAO	middle cerebral artery occlusion
OVX	ovariectomy
CAS	castration
VTN^{-/-}	vitronectin knockout
VTN^{+/+}	vitronectin wildtype
i.v.	intravenous
PBS	phosphate buffer solution
DAB	diaminobenzidine
d	day
h	hour

REFERENCES

- Arvidsson A, Collin T, Kirik D, Kokaia Z, Lindvall O, 2002 Neuronal replacement from endogenous precursors in the adult brain after stroke. *Nat Med* 8, 963–970. [PubMed: 12161747]
- Banner LR, Moayeri NN, Patterson PH, 1997 Leukemia inhibitory factor is expressed in astrocytes following cortical brain injury. *Exp Neurol* 147, 1–9. [PubMed: 9294397]
- Bauer S, Kerr BJ, Patterson PH, 2007 The neuropoietic cytokine family in development, plasticity, disease and injury. *Nat Rev Neurosci* 8, 221–232. [PubMed: 17311007]
- Bauer S, Patterson PH, 2006 Leukemia inhibitory factor promotes neural stem cell self-renewal in the adult brain. *J Neurosci* 26, 12089–12099. [PubMed: 17108182]
- Berti R, Williams AJ, Moffett JR, Hale SL, Velarde LC, Elliott PJ, Yao C, Dave JR, Tortella FC, 2002 Quantitative real-time RT-PCR analysis of inflammatory gene expression associated with ischemia-reperfusion brain injury. *J Cereb Blood Flow Metab* 22, 1068–1079. [PubMed: 12218412]

- Bowen KK, Dempsey RJ, Vemuganti R, 2011 Adult interleukin-6 knockout mice show compromised neurogenesis. *Neuroreport* 22, 126–130. [PubMed: 21266900]
- Campbell IL, Abraham CR, Masliah E, Kemper P, Inglis JD, Oldstone MB, Mucke L, 1993 Neurologic disease induced in transgenic mice by cerebral overexpression of interleukin 6. *Proc Natl Acad Sci U S A* 90, 10061–10065. [PubMed: 7694279]
- Cook DJ, Nguyen C, Chun HN, ILL, Chiu AS, Machnicki M, Zarebinski TI, Carmichael ST, 2017 Hydrogel-delivered brain-derived neurotrophic factor promotes tissue repair and recovery after stroke. *J Cereb Blood Flow Metab* 37, 1030–1045. [PubMed: 27174996]
- Covey MV, Loporchio D, Buono KD, Levison SW, 2011 Opposite effect of inflammation on subventricular zone versus hippocampal precursors in brain injury. *Ann Neurol* 70, 616–626. [PubMed: 21710624]
- del Zoppo GJ, Frankowski H, Gu YH, Osada T, Kanazawa M, Milner R, Wang X, Hosomi N, Mabuchi T, Koziol JA, 2012 Microglial cell activation is a source of metalloproteinase generation during hemorrhagic transformation. *J Cereb Blood Flow Metab* 32, 919–932. [PubMed: 22354151]
- del Zoppo GJ, Milner R, Mabuchi T, Hung S, Wang X, Berg GI, Koziol JA, 2007 Microglial activation and matrix protease generation during focal cerebral ischemia. *Stroke* 38, 646–651. [PubMed: 17261708]
- Ekdahl CT, Claassen JH, Bonde S, Kokaia Z, Lindvall O, 2003 Inflammation is detrimental for neurogenesis in adult brain. *Proc Natl Acad Sci U S A* 100, 13632–13637. [PubMed: 14581618]
- Emsley JG, Hagg T, 2003 Endogenous and exogenous ciliary neurotrophic factor enhances forebrain neurogenesis in adult mice. *Exp Neurol* 183, 298–310. [PubMed: 14552871]
- Erta M, Giral M, Jimenez S, Molinero A, Comes G, Hidalgo J, 2016 Astrocytic IL-6 Influences the Clinical Symptoms of EAE in Mice. *Brain Sci* 6.
- Erta M, Quintana A, Hidalgo J, 2012 Interleukin-6, a major cytokine in the central nervous system. *Int J Biol Sci* 8, 1254–1266. [PubMed: 23136554]
- Giancotti FG, Ruoslahti E, 1999 Integrin signaling. *Science* 285, 1028–1032. [PubMed: 10446041]
- Gotts JE, Chesselet MF, 2005a Mechanisms of subventricular zone expansion after focal cortical ischemic injury. *J Comp Neurol* 488, 201–214. [PubMed: 15924343]
- Gotts JE, Chesselet MF, 2005b Migration and fate of newly born cells after focal cortical ischemia in adult rats. *J Neurosci Res* 80, 160–171. [PubMed: 15751027]
- Gregg C, Weiss S, 2005 CNTF/LIF/gp130 receptor complex signaling maintains a VZ precursor differentiation gradient in the developing ventral forebrain. *Development* 132, 565–578. [PubMed: 15634701]
- He L, Vanlandewijck M, Raschperger E, Andaloussi Mae M, Jung B, Lebouvier T, Ando K, Hofmann J, Keller A, Betsholtz C, 2016 Analysis of the brain mural cell transcriptome. *Sci Rep* 6, 35108. [PubMed: 27725773]
- Heldmann U, Mine Y, Kokaia Z, Ekdahl CT, Lindvall O, 2011 Selective depletion of Mac-1-expressing microglia in rat subventricular zone does not alter neurogenic response early after stroke. *Exp Neurol* 229, 391–398. [PubMed: 21419118]
- Humphries JD, Byron A, Humphries MJ, 2006 Integrin ligands at a glance. *J Cell Sci* 119, 3901–3903. [PubMed: 16988024]
- Iosif RE, Ahlenius H, Ekdahl CT, Darsalia V, Thored P, Jovinge S, Kokaia Z, Lindvall O, 2008 Suppression of stroke-induced progenitor proliferation in adult subventricular zone by tumor necrosis factor receptor 1. *J Cereb Blood Flow Metab* 28, 1574–1587. [PubMed: 18493257]
- Jia C, Brown RW, Malone HM, Burgess KC, Gill WD, Keasey MP, Hagg T, 2019a Ciliary neurotrophic factor is a key sex-specific regulator of depressive-like behavior in mice. *Psychoneuroendocrinology* 100, 96–105. [PubMed: 30299260]
- Jia C, Hegg CC, 2015 Effect of IP3R3 and NPY on age-related declines in olfactory stem cell proliferation. *Neurobiol Aging* 36, 1045–1056. [PubMed: 25482245]
- Jia C, Keasey MP, Lovins C, Hagg T, 2018 Inhibition of astrocyte FAK-JNK signaling promotes subventricular zone neurogenesis through CNTF. *Glia* 66, 2456–2469. [PubMed: 30500112]
- Jia C, Keasey MP, Malone HM, Lovins C, Sante RR, Razskazovskiy V, Hagg T, 2019b Vitronectin from brain pericytes promotes adult forebrain neurogenesis by stimulating CNTF. *Exp Neurol* 312, 20–32. [PubMed: 30408465]

- Kang SS, Keasey MP, Arnold SA, Reid R, Gerald J, Hagg T, 2013 Endogenous CNTF mediates stroke-induced adult CNS neurogenesis in mice. *Neurobiol Dis* 49, 68–78. [PubMed: 22960105]
- Kang SS, Keasey MP, Cai J, Hagg T, 2012 Loss of neuron-astroglial interaction rapidly induces protective CNTF expression after stroke in mice. *J Neurosci* 32, 9277–9287. [PubMed: 22764235]
- Kazanis I, Feichtner M, Lange S, Rotheneichner P, Hainzl S, Oller M, Schallmoser K, Rohde E, Reitsamer HA, Couillard-Despres S, Bauer HC, Franklin RJ, Aigner L, Rivera FJ, 2015 Lesion-induced accumulation of platelets promotes survival of adult neural stem / progenitor cells. *Exp Neurol* 269, 75–89. [PubMed: 25819103]
- Keasey MP, Jia C, Pimentel LF, Sante RR, Lovins C, Hagg T, 2018 Blood vitronectin is a major activator of LIF and IL-6 in the brain through integrin-FAK and uPAR signaling. *J Cell Sci* 131.
- Kernie SG, Parent JM, 2010 Forebrain neurogenesis after focal Ischemic and traumatic brain injury. *Neurobiol Dis* 37, 267–274. [PubMed: 19909815]
- Kim JY, Casaccia-Bonnel P, 2009 Interplay of hormones and p53 in modulating gender dimorphism of subventricular zone cell number. *J Neurosci Res* 87, 3297–3305. [PubMed: 19025772]
- Lambertsen KL, Biber K, Finsen B, 2012 Inflammatory cytokines in experimental and human stroke. *J Cereb Blood Flow Metab* 32, 1677–1698. [PubMed: 22739623]
- Lichtenwalner RJ, Parent JM, 2006 Adult neurogenesis and the ischemic forebrain. *J Cereb Blood Flow Metab* 26, 1–20. [PubMed: 15959458]
- Lin R, Cai J, Kenyon L, Iozzo R, Rosenwasser R, Iacovitti L, 2019 Systemic Factors Trigger Vasculature Cells to Drive Notch Signaling and Neurogenesis in Neural Stem Cells in the Adult Brain. *Stem Cells* 37, 395–406. [PubMed: 30431198]
- Lin R, Cai J, Nathan C, Wei X, Schleidt S, Rosenwasser R, Iacovitti L, 2015 Neurogenesis is enhanced by stroke in multiple new stem cell niches along the ventricular system at sites of high BBB permeability. *Neurobiol Dis* 74, 229–239. [PubMed: 25484283]
- Lin R, Lang M, Heinsinger N, Stricsek G, Zhang J, Iozzo R, Rosenwasser R, Iacovitti L, 2018 Stepwise impairment of neural stem cell proliferation and neurogenesis concomitant with disruption of blood-brain barrier in recurrent ischemic stroke. *Neurobiol Dis* 115, 49–58. [PubMed: 29605425]
- Liu Z, Chopp M, 2016 Astrocytes, therapeutic targets for neuroprotection and neurorestoration in ischemic stroke. *Prog Neurobiol* 144, 103–120. [PubMed: 26455456]
- Lominadze D, Dean WL, Tyagi SC, Roberts AM, 2010 Mechanisms of fibrinogen-induced microvascular dysfunction during cardiovascular disease. *Acta Physiol (Oxf)* 198, 1–13.
- Meng C, Zhang JC, Shi RL, Zhang SH, Yuan SY, 2015 Inhibition of interleukin-6 abolishes the promoting effects of pair housing on post-stroke neurogenesis. *Neuroscience* 307, 160–170. [PubMed: 26327363]
- Milner R, Crocker SJ, Hung S, Wang X, Frausto RF, del Zoppo GJ, 2007 Fibronectin- and vitronectin-induced microglial activation and matrix metalloproteinase-9 expression is mediated by integrins alpha5beta1 and alpha5beta5. *J Immunol* 178, 8158–8167. [PubMed: 17548654]
- Mizrak D, Levitin HM, Delgado AC, Crotet V, Yuan J, Chaker Z, Silva-Vargas V, Sims PA, Doetsch F, 2019 Single-Cell Analysis of Regional Differences in Adult V-SVZ Neural Stem Cell Lineages. *Cell Rep* 26, 394–406 e395. [PubMed: 30625322]
- Monje ML, Toda H, Palmer TD, 2003 Inflammatory blockade restores adult hippocampal neurogenesis. *Science* 302, 1760–1765. [PubMed: 14615545]
- Mudo G, Belluardo N, Mauro A, Fuxe K, 2007 Acute intermittent nicotine treatment induces fibroblast growth factor-2 in the subventricular zone of the adult rat brain and enhances neuronal precursor cell proliferation. *Neuroscience* 145, 470–483. [PubMed: 17241745]
- Ohab JJ, Carmichael ST, 2008 Poststroke neurogenesis: emerging principles of migration and localization of immature neurons. *Neuroscientist* 14, 369–380. [PubMed: 18024854]
- Ohab JJ, Fleming S, Blesch A, Carmichael ST, 2006 A neurovascular niche for neurogenesis after stroke. *J Neurosci* 26, 13007–13016. [PubMed: 17167090]
- Ourednik J, Ourednik V, Lynch WP, Schachner M, Snyder EY, 2002 Neural stem cells display an inherent mechanism for rescuing dysfunctional neurons. *Nat Biotechnol* 20, 1103–1110. [PubMed: 12379867]

- Parent JM, Vexler ZS, Gong C, Derugin N, Ferriero DM, 2002 Rat forebrain neurogenesis and striatal neuron replacement after focal stroke. *Ann Neurol* 52, 802–813. [PubMed: 12447935]
- Pitman M, Emery B, Binder M, Wang S, Butzkueven H, Kilpatrick TJ, 2004 LIF receptor signaling modulates neural stem cell renewal. *Mol Cell Neurosci* 27, 255–266. [PubMed: 15519241]
- Quintana A, Giralt M, Rojas S, Penkowa M, Campbell IL, Hidalgo J, Molinero A, 2005 Differential role of tumor necrosis factor receptors in mouse brain inflammatory responses in cryolesion brain injury. *J Neurosci Res* 82, 701–716. [PubMed: 16267827]
- Shimazaki T, Shingo T, Weiss S, 2001 The ciliary neurotrophic factor/leukemia inhibitory factor/gp130 receptor complex operates in the maintenance of mammalian forebrain neural stem cells. *J Neurosci* 21, 7642–7653. [PubMed: 11567054]
- Shruster A, Ben-Zur T, Melamed E, Offen D, 2012 Wnt signaling enhances neurogenesis and improves neurological function after focal ischemic injury. *PLoS One* 7, e40843. [PubMed: 22815838]
- Storer MA, Gallagher D, Fatt MP, Simonetta JV, Kaplan DR, Miller FD, 2018 Interleukin-6 Regulates Adult Neural Stem Cell Numbers during Normal and Abnormal Post-natal Development. *Stem Cell Reports* 10, 1464–1480. [PubMed: 29628394]
- Strecker JK, Minnerup J, Gess B, Ringelstein EB, Schabitz WR, Schilling M, 2011 Monocyte chemoattractant protein-1-deficiency impairs the expression of IL-6, IL-1beta and G-CSF after transient focal ischemia in mice. *PLoS One* 6, e25863. [PubMed: 22031820]
- Suzuki S, Gerhold LM, Bottner M, Rau SW, Dela Cruz C, Yang E, Zhu H, Yu J, Cashion AB, Kindy MS, Merchenthaler I, Gage FH, Wise PM, 2007 Estradiol enhances neurogenesis following ischemic stroke through estrogen receptors alpha and beta. *J Comp Neurol* 500, 1064–1075. [PubMed: 17183542]
- Suzuki S, Tanaka K, Suzuki N, 2009 Ambivalent aspects of interleukin-6 in cerebral ischemia: inflammatory versus neurotrophic aspects. *J Cereb Blood Flow Metab* 29, 464–479. [PubMed: 19018268]
- Tatar C, Bessert D, Tse H, Skoff RP, 2013 Determinants of central nervous system adult neurogenesis are sex, hormones, mouse strain, age, and brain region. *Glia* 61, 192–209. [PubMed: 23027402]
- Taylor RA, Sansing LH, 2013 Microglial responses after ischemic stroke and intracerebral hemorrhage. *Clin Dev Immunol* 2013, 746068. [PubMed: 24223607]
- Thored P, Heldmann U, Gomes-Leal W, Gisler R, Darsalia V, Taneera J, Nygren JM, Jacobsen SE, Ekdahl CT, Kokaia Z, Lindvall O, 2009 Long-term accumulation of microglia with proneurogenic phenotype concomitant with persistent neurogenesis in adult subventricular zone after stroke. *Glia* 57, 835–849. [PubMed: 19053043]
- Tonchev AB, Yamashima T, Zhao L, Okano HJ, Okano H, 2003 Proliferation of neural and neuronal progenitors after global brain ischemia in young adult macaque monkeys. *Mol Cell Neurosci* 23, 292–301. [PubMed: 12812760]
- Tsai PT, Ohab JJ, Kertesz N, Groszer M, Matter C, Gao J, Liu X, Wu H, Carmichael ST, 2006 A critical role of erythropoietin receptor in neurogenesis and post-stroke recovery. *J Neurosci* 26, 1269–1274. [PubMed: 16436614]
- Turnquist C, Horikawa I, Foran E, Major EO, Vojtesek B, Lane DP, Lu X, Harris BT, Harris CC, 2016 p53 isoforms regulate astrocyte-mediated neuroprotection and neurodegeneration. *Cell Death Differ* 23, 1515–1528. [PubMed: 27104929]
- Vallieres L, Campbell IL, Gage FH, Sawchenko PE, 2002 Reduced hippocampal neurogenesis in adult transgenic mice with chronic astrocytic production of interleukin-6. *J Neurosci* 22, 486–492. [PubMed: 11784794]
- Van Wagoner NJ, Benveniste EN, 1999 Interleukin-6 expression and regulation in astrocytes. *J Neuroimmunol* 100, 124–139. [PubMed: 10695723]
- Verkhatsky A, Nedergaard M, 2018 Physiology of Astroglia. *Physiol Rev* 98, 239–389. [PubMed: 29351512]
- Wang X, Mao X, Xie L, Greenberg DA, Jin K, 2009 Involvement of Notch1 signaling in neurogenesis in the subventricular zone of normal and ischemic rat brain in vivo. *J Cereb Blood Flow Metab* 29, 1644–1654. [PubMed: 19536070]
- Wiltrout C, Lang B, Yan Y, Dempsey RJ, Vemuganti R, 2007 Repairing brain after stroke: a review on post-ischemic neurogenesis. *Neurochem Int* 50, 1028–1041. [PubMed: 17531349]

- Yamashima T, Tonchev AB, Vachkov IH, Popivanova BK, Seki T, Sawamoto K, Okano H, 2004 Vascular adventitia generates neuronal progenitors in the monkey hippocampus after ischemia. *Hippocampus* 14, 861–875. [PubMed: 15382256]
- Yan YP, Sailor KA, Vemuganti R, Dempsey RJ, 2006 Insulin-like growth factor-1 is an endogenous mediator of focal ischemia-induced neural progenitor proliferation. *Eur J Neurosci* 24, 45–54. [PubMed: 16882007]
- Yang P, Arnold SA, Habas A, Hetman M, Hagg T, 2008 Ciliary neurotrophic factor mediates dopamine D2 receptor-induced CNS neurogenesis in adult mice. *J Neurosci* 28, 2231–2241. [PubMed: 18305256]
- Zhang R, Zhang Z, Chopp M, 2016 Function of neural stem cells in ischemic brain repair processes. *J Cereb Blood Flow Metab* 36, 2034–2043. [PubMed: 27742890]
- Zhang W, Cheng J, Vagnerova K, Ivashkova Y, Young J, Cornea A, Grafe MR, Murphy SJ, Hurn PD, Brambrink AM, 2014 Effects of androgens on early post-ischemic neurogenesis in mice. *Transl Stroke Res* 5, 301–311. [PubMed: 24323721]

Highlights

- Vitronectin (VTN) leaks from blood into the subventricular zone (SVZ) of adult mice after ischemic stroke.
- VTN inhibits stroke-induced SVZ neurogenesis in females, but not males, by promoting acute expression of SVZ IL-6.
- The female-specific VTN-induced IL-6 was through activation of FAK signaling but not due to gonadal hormones.
- Astrocytic FAK plays a role in repressing stroke-induced IL-6 in females only.
- VTN or VTN signaling may be a good targets for promoting neurogenesis for neuroprotection and cell replacement in females.

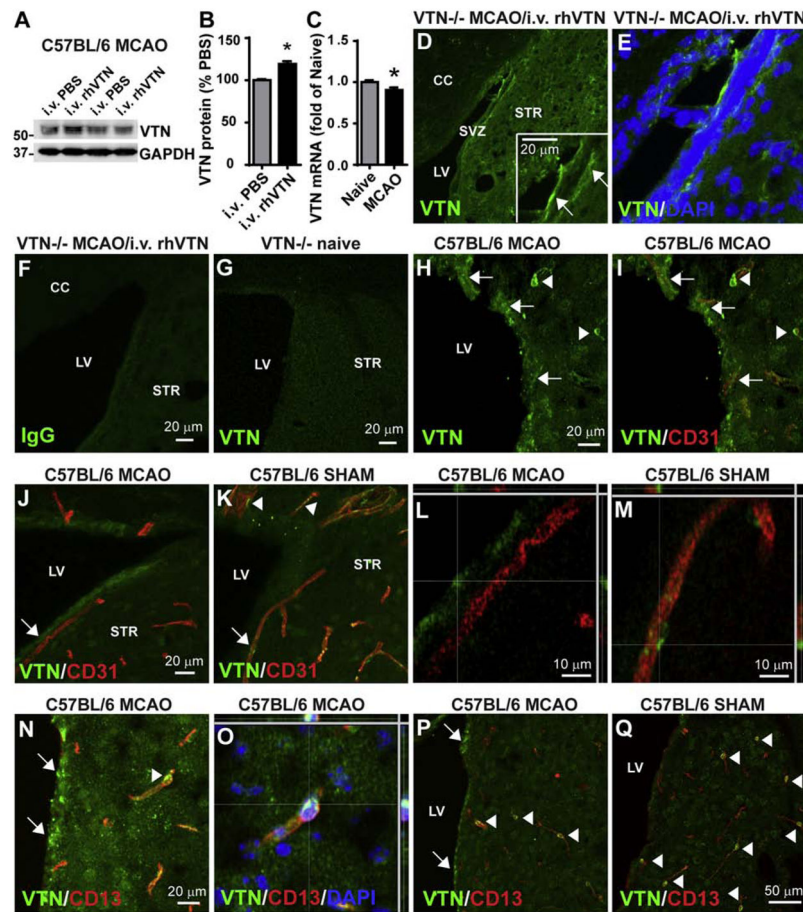


Figure 1. Blood VTN leaks into the SVZ following MCAO.

A) C57BL/6 mice injected i.v. with rhVTN at 24 h following MCAO show an increase of VTN protein in the SVZ 4 h later compared to PBS-injected mice. Different lanes in the representative western blot indicate SVZ samples from individual mice injected with PBS or rhVTN. **B)** Densitometry analysis from western blots of 3 independent gels and with $n = 3$ mice/group, * $p < 0.05$ (T test). **C)** MCAO reduced VTN mRNA in the SVZ of C57BL/6 mice at 24 h. $N = 3$ and 5 mice. * $p < 0.05$ (T-test). **D,E)** Deposits of i.v. injected rhVTN was detectable in the SVZ of VTN $^{-/-}$ mice by immunostaining. The insert in (D) is a higher magnification image and arrows indicate leaked VTN. No positive immunostaining was seen when the primary antibody was replaced by isotype IgG (**F**) or in the SVZ of naïve VTN $^{-/-}$ mice stained with VTN antibody (**G**). **H)** VTN deposits (green, indicated by arrows) were also detected in the SVZ of wildtype C57BL/6 mice 24 h following MCAO and were present around microvessels identified with the endothelial cell marker CD 31 (red, **I**). Pericytes apposing blood vessels in the brain expressed VTN (arrowheads in **K**), as also shown by co-localization with the pericyte marker CD13 (red, **N**, arrowhead, shown in a confocal image in **O**). The number of VTN-positive pericytes was reduced at 24 h following MCAO (**J,P**) compared to sham-operated mice (**K,Q**). Arrowheads indicate VTN-positive (green) pericytes expressing CD13 (red). Arrows indicate leaked VTN in the SVZ. Scale bars are as indicated, CC, corpus callosum, LV, lateral ventricle, STR, striatum.

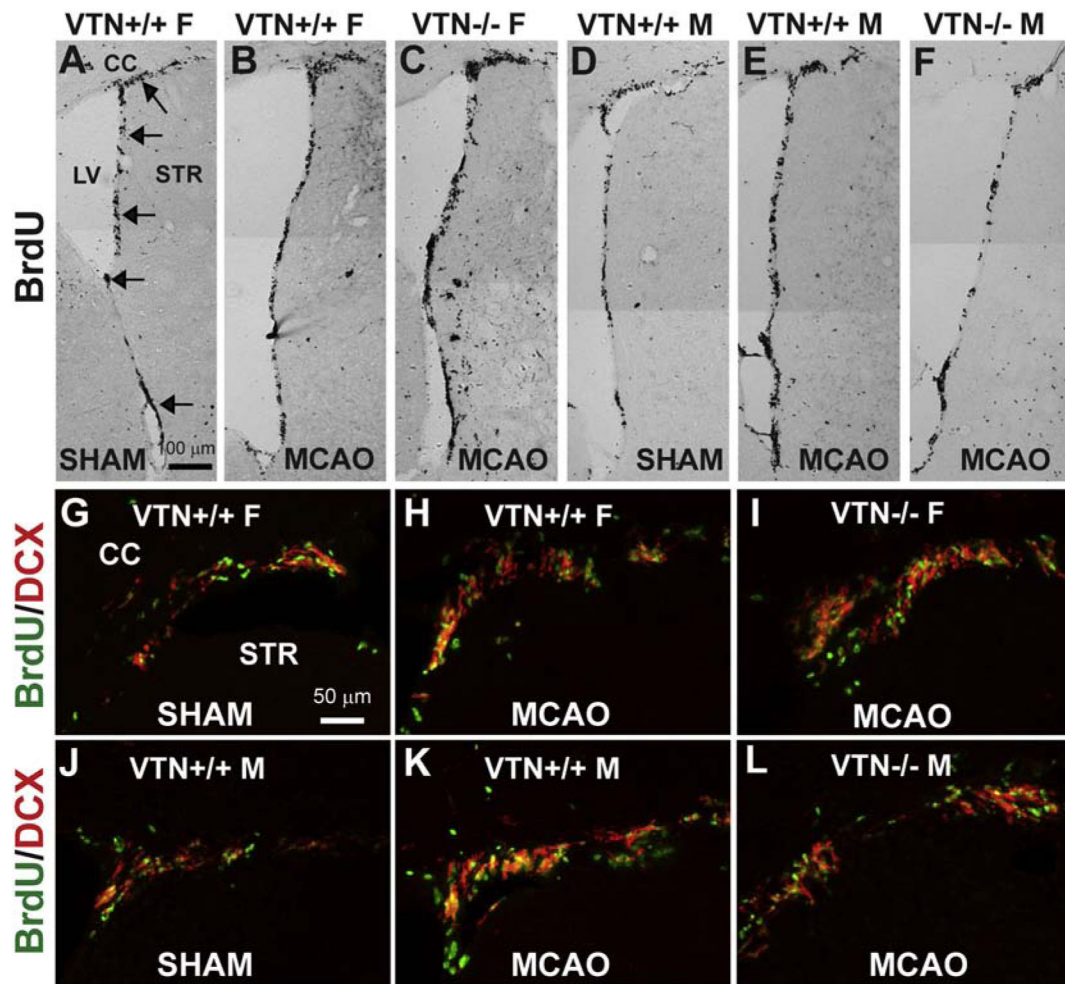


Figure 2. MCAO-induced SVZ proliferation and neurogenesis is increased even more in female, but not male, VTN^{-/-} mice.

Female and male VTN^{+/+} and VTN^{-/-} mice received a 30 min MCAO and analyzed at 14 d, with BrdU given over the last 3 days. Representative images of BrdU⁺ nuclei in the SVZ show that, compared to sham-operated females (A), MCAO causes an increase in VTN^{+/+} females (B) and even more so in VTN^{-/-} females (C). In males, the increase compared to shams (D) was similar in VTN^{+/+} (E) and VTN^{-/-} (F). Arrows indicate the SVZ. F, female, M, male, CC, corpus callosum, LV = lateral ventricle, STR, striatum, scale bar = 100 μm. Immunostaining for BrdU and the neuroblast marker, DCX, confirmed that the increased proliferation led to formation of new neuroblasts, i.e., neurogenesis in females (G-I) and males (J-L) mice. Scale bar = 50 μm.

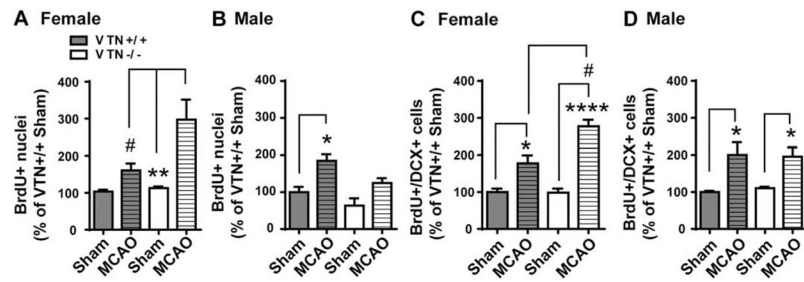


Figure 3. VTN^{-/-} female, but not male, mice have enhanced MCAO-induced SVZ neurogenesis. Unbiased stereological counts of BrdU⁺ nuclei were expressed as a percentage of sham operated VTN^{+/+} mice. This showed that the MCAO-induced proliferation in the SVZ occurred both in females (**A**) and male (**B**), but that only female VTN^{-/-} mice had an even greater response. BrdU⁺/DCX⁺ cell counts in the SVZ of females (**C**) and males (**D**) confirmed that this was also true for neurogenesis. N = 4, 7, 4 and 4 mice in females and N = 5, 3, 7 and 3 in males. * p<0.05, ** p<0.01, **** p<0.0001, Sham vs. MCAO, # p<0.05, VTN^{+/+} vs. VTN^{-/-} in MCAO mice (Two-way ANOVA followed by post hoc Tukey multiple comparisons).

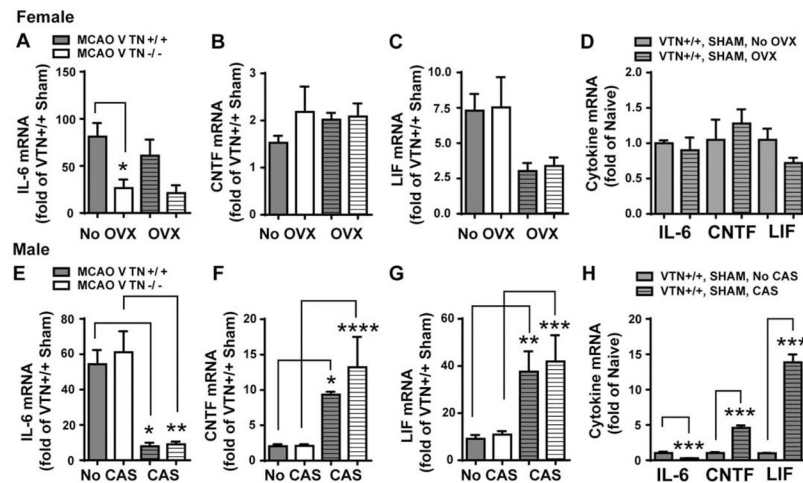


Figure 4. Only VTN^{-/-} females have lower IL-6 following MCAO but in a gonadal hormone-independent manner.

Female and male VTN^{+/+} and VTN^{-/-} mice were ovariectomized (OVX) or castrated (CAS), respectively. Two weeks later, they received a sham operation or a 30 min MCAO. After 24 h, the cytokine mRNA in the SVZ were measured by RT-qPCR and expressed as a fold change compared to VTN^{+/+} shams within each sex. **A**) In female mice without OVX (first two columns), MCAO-induced IL-6 was substantially lower in VTN^{-/-} mice compared to VTN^{+/+} mice, indicating that VTN induces IL-6 following MCAO in female mice. The MCAO-induced CNTF (**B**) and LIF (**C**) were comparable between VTN^{+/+} and VTN^{-/-} females. After OVX, the lower MCAO-induced increase in IL-6 of VTN^{-/-} females (**A**) was not different from the lower levels seen in VTN^{-/-} females without OVX, suggesting that ovary hormones do not contribute to VTN-induced IL-6 following MCAO. Levels of CNTF (**B**) and LIF (**C**) were also similar between VTN^{+/+} and VTN^{-/-} females after OVX alone. OVX itself did not significantly alter IL-6, CNTF and LIF mRNA in MCAO sham-operated mice compared to no OVX (**D**). In males without CAS (first two columns) and with CAS (the last two columns), MCAO-induced IL-6 (**E**), CNTF (**F**) and LIF (**G**) were comparable between VTN^{+/+} and VTN^{-/-} mice, suggesting that male sex hormones do not affect the VTN regulation of these cytokines following MCAO. However, CAS substantially reduced IL-6 (**E**) and increased CNTF (**F**) and LIF (**G**) following MCAO. **H**) CAS-induced changes in these cytokines were also observed in MCAO sham-operated mice. N = 7, 6, 9 and 10 in female mice and 10, 12, 4 and 5 in male mice for MCAO. N = 4 and 5 mice in female sham, N = 3 and 5 mice in male sham. * p<0.05, ** p<0.01, *** p<0.001, **** p<0.0001 (Two-way ANOVA followed by post hoc Tukey multiple comparisons).

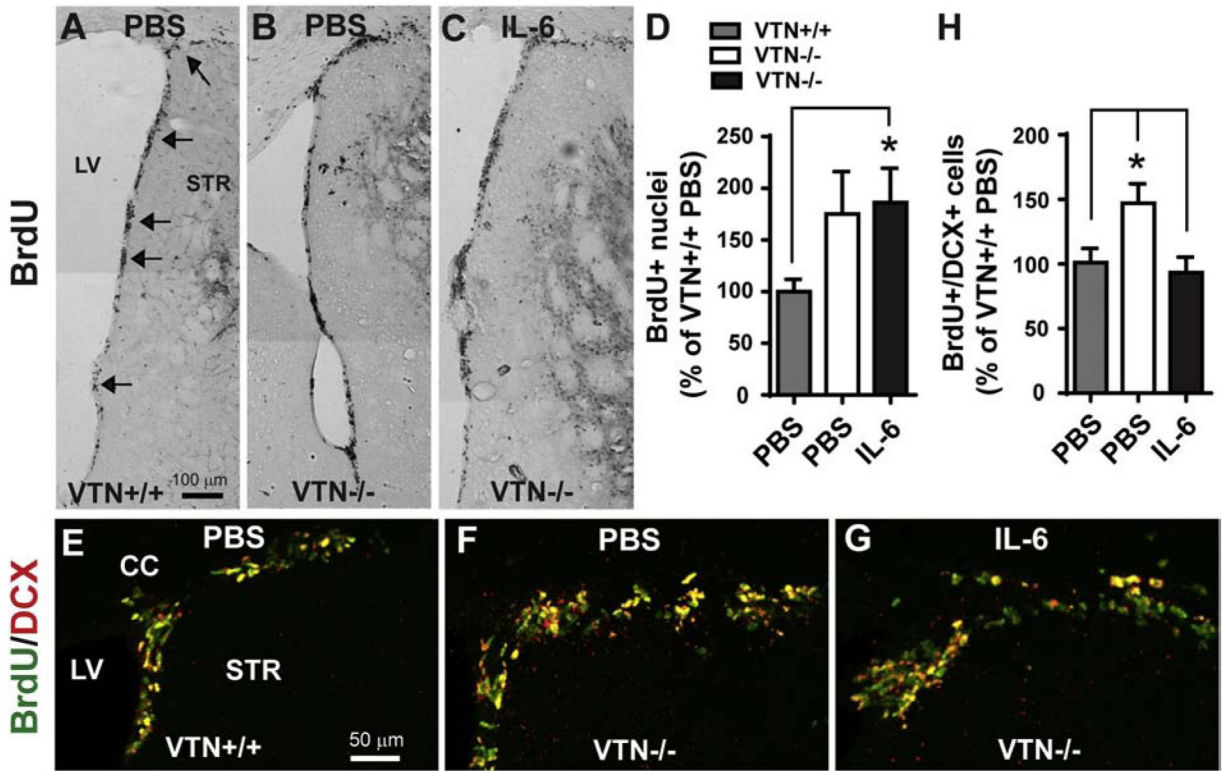


Figure 5. IL-6 blocks the female-specific VTN^{-/-} phenotype of increased MCAO-induced neurogenesis.

Female VTN^{+/+} and VTN^{-/-} mice were injected with PBS or IL-6 (100 ng) into the striatum next to the SVZ immediately prior to MCAO. BrdU were given the last 50 h before tissue collection at 14 days after MCAO. **A-C)** Representative images show that BrdU⁺ nuclei in the SVZ are more numerous in VTN^{-/-} mice after PBS or IL-6 injection than in VTN^{+/+} mice after PBS injection. Arrows indicate the SVZ. LV, lateral ventricle, STR, striatum, scale bar = 100 μ m. **D)** Unbiased stereological counting of BrdU⁺ nuclei in the SVZ were expressed as a percentage of PBS-injected VTN^{+/+} mice. This confirmed that VTN^{-/-} mice have more proliferation after both PBS and IL-6 injection. N = 7, 3 and 6 mice. **E-G)** Representative images show that BrdU⁺/DCX⁺ cells in the dorsolateral SVZ of VTN^{+/+} and VTN^{-/-} mice. The increase in VTN^{-/-} mice seemed smaller after IL-6 compared to PBS injection. Scale bar = 50 μ m. **H)** Quantification of BrdU⁺/DCX⁺ cells confirmed that VTN^{-/-} mice have more neurogenesis than VTN^{+/+} mice, which was blocked by IL-6. N = 9, 3 and 6 mice. * p<0.05 (One-way ANOVA followed by post hoc Bonferroni multiple comparisons).

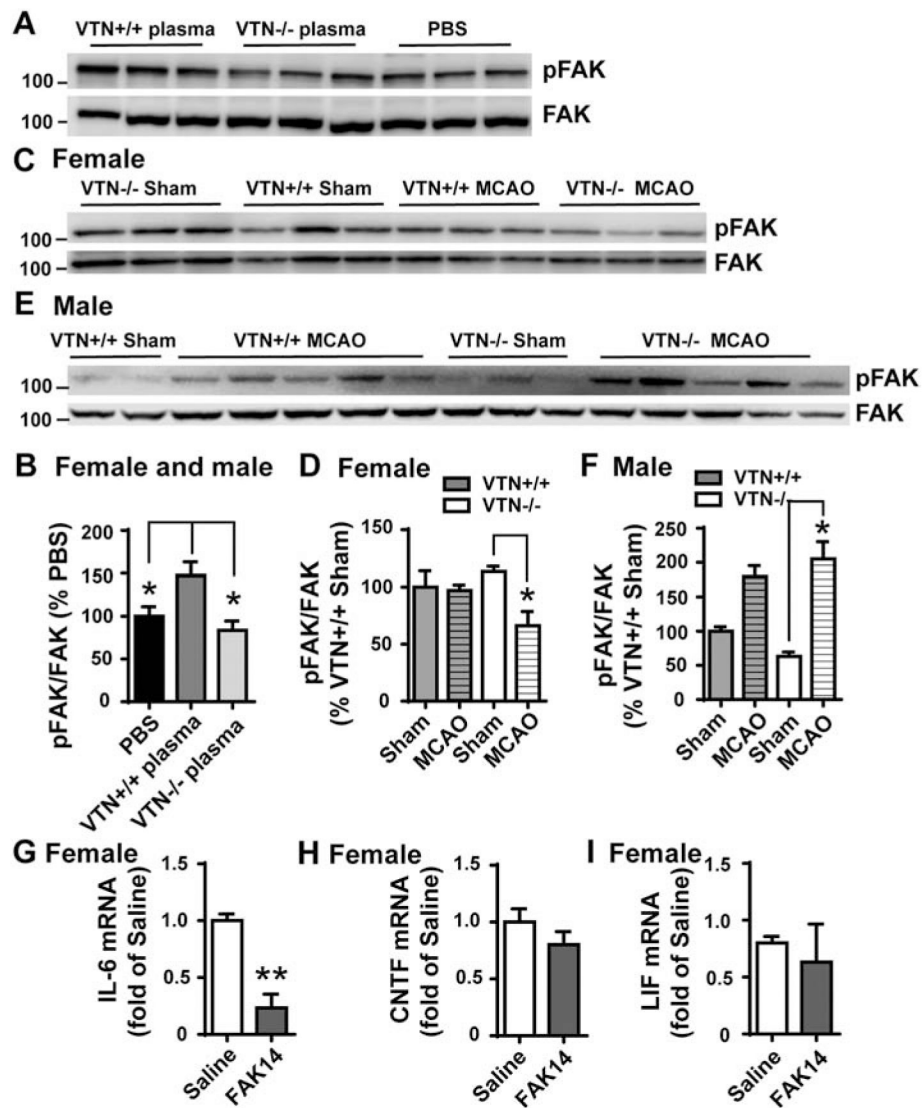


Figure 6. Plasma VTN activates FAK and IL-6 following stroke in the SVZ of female mice.

A) In naïve mice, plasma from VTN^{+/+}, but not VTN^{-/-}, mice increased pFAK in the SVZ compared to PBS injected 24 h before into the striatum, as shown in a representative western blot and densitometry (**B**). **C)** pFAK was reduced 24 h after MCAO in the SVZ of VTN^{-/-} female mice compare to their sham controls as shown by a representative western blot and densitometry (**D**). MCAO did not induce pFAK in VTN^{+/+} females following MCAO, suggesting that leaked VTN maintains FAK activation. **E,F)** In males, the levels of pFAK were increased to the same extent in VTN^{+/+} and VTN^{-/-} mice following MCAO, suggesting VTN does not activate FAK in males after a stroke. N = 3, 5, 4 and 6 mice in females, N = 4, 8, 3 and 12 mice in males. * p<0.05 (Two-way ANOVA followed by post hoc Tukey multiple comparisons). **G-I)** Female C57BL/6 mice with an MCAO were injected i.p. with saline or the FAK inhibitor FAK14 (3 mg/kg) at 6 h. At 24 h after MCAO, FAK14 reduced IL-6 (**G**) mRNA expression in the SVZ, without altering CNTF (**H**) and LIF (**I**). N = 3, 4 and 3 mice. ** p<0.01 (T-test).

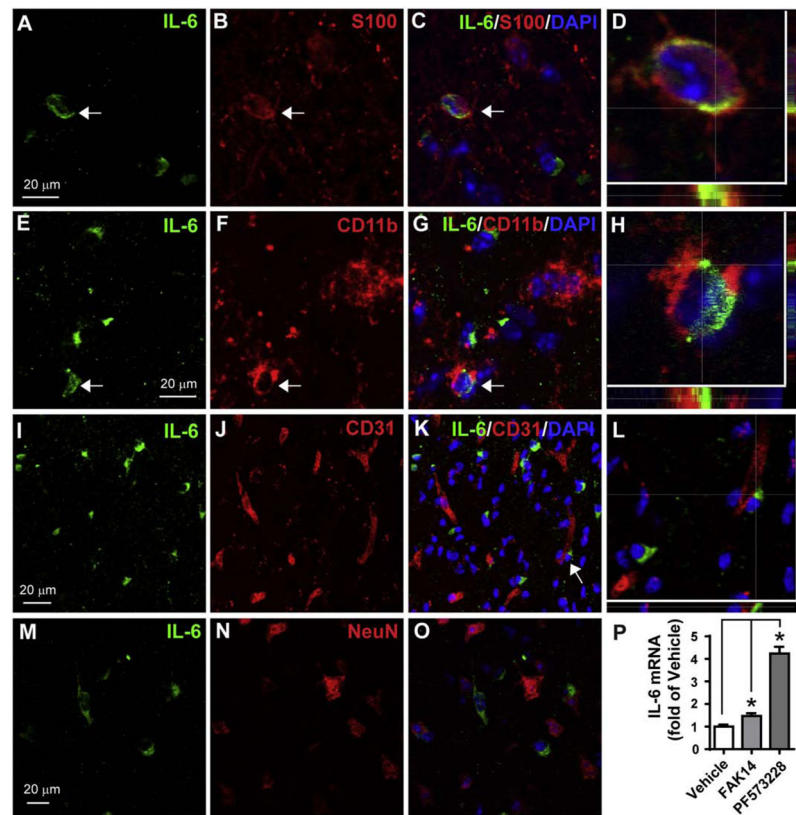


Figure 7. MCAO induces IL-6 protein expression in astrocytes and microglia/macrophages. A 30 min of MCAO was performed in C57BL/6 mice and at 24 h IL-6 was detected in cells by double-immunofluorescent staining in the striatum close to SVZ. **A-C**) IL-6 (green) was colocalized in some astrocytes (arrow) identified with S100 staining (red), which is shown in a confocal image at higher magnification in **(D)**. Nuclei were stained with DAPI (blue). **E-H**) IL-6 (green) was also present in some microglia/macrophages identified by CD11b (red). IL-6 was not present in endothelial cells (CD31, **I-L**) or neurons (NeuN, **M-O**). The areas indicated by arrows in C,G and K are shown with high magnification in D,H and L, respectively. Scale bar = 20 μ m. **P**) Pharmacological inhibition of FAK in mouse primary astrocytes increases IL-6 expression. Mouse primary astrocyte cultures were incubated with vehicle (0.1% DMSO), FAK14 (10 μ M) or PF573228 (10 μ M) for 4 h and then IL-6 mRNA was measured by RT-qPCR. N = 3 independent experiments. * $p < 0.05$ (paired one-way ANOVA followed by post hoc Bonferroni multiple comparisons).

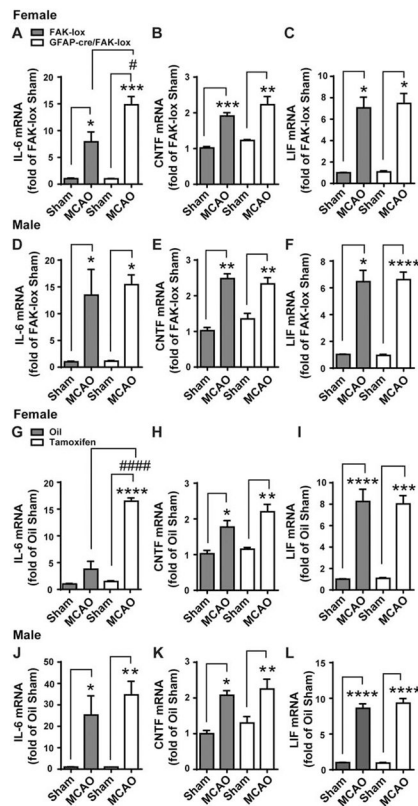


Figure 8. Astrocytic FAK deletion increases MCAO-induced IL-6 in females.

Female and male GFAP-cre/FAK-lox mice were treated for 5 days with tamoxifen to delete FAK in astrocytes. FAK-lox controls were treated the same. Two weeks after the last tamoxifen injection, they received a 30 min MCAO or a sham operation and the levels of cytokine mRNA in the SVZ were measured 24 later. Values were expressed as a fold change compared to sham-operated FAK-lox control mice. **A)** In females, MCAO caused an expected increase of IL-6 in FAK-lox controls (first two columns), and an even greater response in GFAP-cre/FAK-lox (last two columns). MCAO induced CNTF (**B**) and LIF (**C**) to the same extent in FAK-lox and GFAP-cre/FAK-lox females. In male mice, MCAO increased IL-6 (**D**), CNTF (**E**) and LIF (**F**) to the same extent in both FAK-lox and GFAP-cre/FAK-lox mice. $N = 6, 9, 4$ and 7 mice in females and $N = 4, 5, 4$ and 6 mice in males. To confirm that the effect of astrocyte FAK deletion were not due to lasting effects of tamoxifen, another set of GFAP-cre/FAK-lox mice was treated with oil or tamoxifen for 5 d and with an MCAO 14 d later. At 24 h following MCAO, SVZ mRNA expression was measured and calculated as a fold change from oil-treated sham operated mice within each sex. **G)** MCAO induced IL-6 was further increased with tamoxifen compared to oil control, which is consistent with data in (A). MCAO-induced CNTF (**H**) and LIF (**I**) were comparable between oil and tamoxifen treatment and within a similar range as seen in (B) and (C). In male mice, there were no differences of MCAO-induced IL-6 (**J**), CNTF (**K**) and LIF (**L**) between oil and tamoxifen-treated mice. $N = 4, 4, 4$ and 3 mice in females and $N = 3, 4, 5$ and 4 mice in males. * $p < 0.05$, # $p < 0.05$, ** $p < 0.01$, *** $p < 0.001$, **** $p < 0.0001$ (Two-way ANOVA followed by post hoc Tukey multiple comparisons).

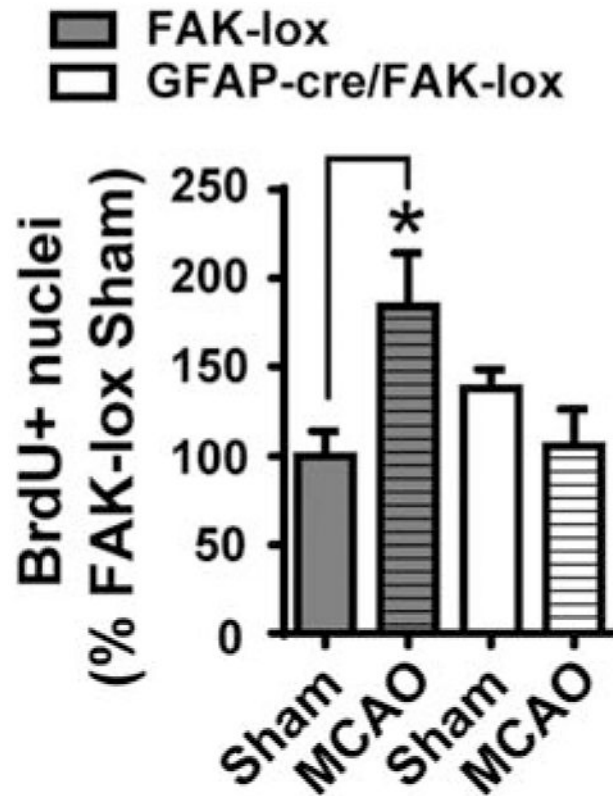


Figure 9. Astrocytic FAK deletion blocks MCAO-induced neurogenesis in the SVZ of females. Female FAK-lox control and GFAP-cre/FAK-lox mice received 5 days of tamoxifen treatment followed by MCAO 14 d later. BrdU was given during the last 50 h prior to tissue collection at 14 d following MCAO. The numbers of BrdU+ nuclei in the SVZ were counted using unbiased stereology and calculated as percent of sham-operated FAK-lox controls. MCAO caused the expected increase in BrdU+ nuclei in FAK-lox mice, but not GFAP-cre/FAK-lox mice, suggesting that selective deletion of FAK in the astrocytes blocks MCAO-induced SVZ neurogenesis. N = 6, 5, 5 and 4 mice. * $p < 0.05$ (Two-way ANOVA followed by post hoc Tukey multiple comparisons).